ORIGINAL ARTICLE

Cardiovascular Magnetic Resonance Imaging-Based Computational Fluid Dynamics/Fluid–Structure Interaction Pilot Study to Detect Early Vascular Changes in Pediatric Patients with Type 1 Diabetes

Margaret M. Samyn · Ronak Dholakia · Hongfeng Wang ·
Jennifer Co-Vu · Ke Yan · Michael E. Widlansky ·
John F. LaDisa · Pippa Simpson · Ramin Alemzadeh

Abstract We hypothesized that pediatric patients with type 1 diabetes have cardiac magnetic resonance (CMR) detectable differences in thoracic aortic wall properties and hemodynamics leading to significant local differences in indices of wall shear stress, when compared with age-matched control subjects without diabetes. Pediatric patients with type 1 diabetes were recruited from Children's Hospital of Wisconsin and compared with controls. All underwent morning CMR scanning, 4-limb blood pressure, brachial artery reactivity testing, and venipuncture. Patient-specific computational fluid dynamics modeling with fluid–structure interaction, based on CMR data, determined regional time-averaged wall shear stress (TAWSS) and oscillatory shear index (OSI). Twenty type 1 diabetic subjects, median age 15.8 years (11.6–18.4) and 8 controls 15.4 years (10.3–18.2) were similar except for higher glucose, hemoglobin A1c, and triglycerides for type 1 diabetic subjects. Lower flow-mediated dilation was seen for those with type 1 diabetes (6.5) versus controls (7.8), $p = 0.036$. For type 1 diabetic subjects, the aorta had more regions with high TAWSS when compared to controls. OSI maps appeared similar. Flow-mediated dilation positively correlated with age at diabetes diagnosis ($r = 0.468$, $p = 0.038$) and hemoglobin A1c ($r = 0.472$, $p = 0.036$), but did not correlate with aortic distensibility, TAWSS, or OSI. TAWSS did not correlate with any clinical parameter for either group. CMR shows regional differences in aortic wall properties for young diabetic patients. Some local differences in wall shear stress indices were also observed, but a longitudinal study is now warranted.

Keywords Diabetes · Magnetic resonance imaging · Pediatrics

M. M. Samyn (✉) · K. Yan · P. Simpson
Department of Pediatrics, Medical College of Wisconsin,
Milwaukee, WI, USA
e-mail: msamyn@chw.org

M. M. Samyn · H. Wang · J. F. LaDisa
Department of Biomedical Engineering, Marquette University,
Milwaukee, WI, USA

R. Dholakia
Stony Brook University Medical Center, Stony Brook, NY, USA

J. Co-Vu
Congenital Heart Center and Department of Pediatrics,
University of Florida College of Medicine, Gainesville, FL, USA

M. E. Widlansky · J. F. LaDisa
Department of Medicine, Medical College of Wisconsin,
Milwaukee, WI, USA

J. F. LaDisa
Biotechnology and Bioengineering Center, Medical College
of Wisconsin, Milwaukee, WI, USA

R. Alemzadeh
Division of Pediatric Endocrinology, University of Illinois at
Chicago, Chicago, IL, USA

Introduction

Cardiovascular disease afflicts greater than 83 million Americans, with coronary heart disease (CHD) affecting more than 15 million Americans [11]. Traditional risk factors for the development of atherosclerosis include diabetes, dyslipidemia, hypertension, obesity, smoking, and sedentary lifestyle [29]. Type 1 diabetes is associated with a fivefold to sevenfold increase in risk of death from coronary heart disease. Patients with type 1 diabetes have been shown to have endothelial dysfunction, the inciting event for atherosclerosis [14]. Endothelial dysfunction and

arterial stiffness are independent predictors of cardiovascular events; improved endothelial function can decrease cardiovascular events [12, 15, 40]. The reduced endothelial function seen in individuals with diabetes allows for premature integration of lipid laden macrophages in the vessel walls. In addition, the hyperglycemic environment seen in diabetic patient results in qualitative changes in low density lipoprotein (LDL) particle size, oxidation, and glycation—all of which are implicated in early increases in carotid artery intimal media thickness and endothelial dysfunction [31, 41].

A special feature of CMR imaging is its ability for tissue discrimination. Clinically, magnetic resonance imaging has been reported in adults to detect atherosclerotic plaques in the thoracic and abdominal aorta with detection of thoracic aortic plaque associated with co-existent coronary artery disease (CAD) [38]. A study of adults with pre-existing plaques revealed time-averaged wall shear stress (TAWSS) flow patterns in a rotating pattern down the thoracic aorta that correlated with the areas of atherosclerotic plaque [46]. A better understanding of the relationship between endothelial shear stress and arterial remodeling and stiffening is needed, as arterial stiffening seems to lie at the heart of atherosclerotic plaque development [44]. While some adult studies exist, magnetic resonance imaging studies examining the vascular health of pediatric subjects, prior to the development of overt atherosclerotic plaque, are not found in the literature.

The purpose of our pilot, prospective study was to determine the feasibility of CMR imaging for evaluation of early vascular changes in a pediatric cohort with type 1 diabetes, who are at increased risk of developing atherosclerosis. We hypothesized that pediatric patients with type 1 diabetes would have CMR detectable differences in thoracic aortic wall properties and hemodynamics leading to local differences in indices of wall shear stress, as quantified by patient-specific computational fluid dynamics (CFD) modeling with fluid–structure interaction, when compared with age-matched control subjects without diabetes. Correlation between CMR data and brachial artery reactivity measures of endothelial function, as well as with other atherosclerotic risk factors, was investigated.

Materials and Methods

Recruitment

Twenty children with type 1 diabetes, aged 12–18 years, were recruited from Children's Hospital of Wisconsin (CHW) Diabetes Clinic, affiliated with the Medical College of Wisconsin. Children with type 1 diabetes were either on multiple daily insulin consisting of bedtime insulin

glargine® and pre-meal aspart® insulin or continuous subcutaneous insulin infusion with insulin aspart®. In addition, eight age-matched control subjects were recruited consecutively from among those patients having clinically indicated CMR scans. Inclusion criteria included pre-pubescent to post-pubescent children/adolescents between 10 and 18 years of age and at least a 2-year history of diabetes. Exclusion criteria included known history of contraindication to CMR examination (i.e., pregnancy as determined by beta human chorionic gonadotrophin (β-hCG), presence of a pacemaker or defibrillator, or claustrophobia), hypercholesterolemia, metabolic syndrome, hypertension, microvascular complications, congenital heart disease (for diabetic study recruits), and family history of hypercholesterolemia or premature cardiovascular disease. Furthermore, control subjects were excluded if taking any lipid lowering, oral hypoglycemic, or antihypertensive medications for more than 1 week. The study protocol was approved by the CHW institutional review board. Informed consent and assent were obtained from the study parents/guardians and subjects.

Study Evaluations

Evaluations included early morning (0630 AM, fasting) CMR scanning using a Siemens 1.5 T Symphony® (Siemens Medical Systems, USA) magnet, with same-day 4-limb blood pressure (BP) assessment (DASH 3000 Vital Signs Monitor, GE Healthcare, Waukesha WI) and morning (0800) brachial artery reactivity testing with high-resolution ultrasound (GE Pro Logiq 500, Waukesha WI). Subjects underwent same-day venipuncture for fasting laboratory assessment (i.e., glucose, hemoglobin A1c, insulin, lipid profile, fibrinogen, homocysteine, high-sensitivity c reactive protein (hs-CRP)) by previously described analytical methods [3]. In addition, chart review allowed extraction of key clinical data including primary and secondary diagnoses, age at diabetes diagnosis, and medication use for type 1 diabetic subjects.

Data Collection

Standard CMR scanning was performed using a Siemens 1.5 T Symphony magnet with study supervised by a qualified pediatric cardiologist, using clinically available pulse sequence software (Siemens Medical Solutions USA, Malvern, PA) with standard calculation of ventricular volumes and flow (Medis®, Leiden, The Netherlands). For this study, the subjects did not receive gadolinium dye, but rather CMR three-dimensional (3D) steady state-free precession (SSFP) images of the arch were obtained from a respiratory navigated sequence (bandwidth 590, matrix 256 × 173, TE 1.86, TR 298, NEX 1, acceptable window

2.5 mm). Phase contrast velocity encoded cine imaging (FOV 256 × 192, slice thickness 5–6 mm, bandwidth 390, TE 3.26–4.1, TR 27.75–46, ETL 1, NEX 3) of flow volume was determined for the ascending and descending aorta, as well as for each brachiocephalic vessel to be used in later CFD modeling. Care was taken during flow assessment to select similar flow imaging planes for each subject; thus, a plane perpendicular to AAo flow, at the level of the pulmonary arterial bifurcation, was prescribed for AAo flow assessment and similarly a separate plane for the DAo flow assessment was undertaken at the level of branch PAs. Aortic distensibility was calculated from measured BP and cross-sectional phase contrast magnitude images of the ascending aorta, descending thoracic aorta, and descending thoracic aorta at the diaphragm, using the formula [43]:

$$\text{Aortic distensibility} = \frac{[(\text{Aortic cross sectional area})\max - (\text{Aortic cross sectional area})\min]}{[(\text{Aortic cross sectional area})\min \times \text{pulse pressure}]}.$$

Reactive hyperemia (i.e., flow-mediated dilation, FMD) was assessed for each subject after being in the supine position for 10 min at a stable room temperature [3, 4]. The methods for determining, analyzing, and reporting the FMD percentage (FMD%) in the brachial artery, as a surrogate of endothelial function, were performed using mobile equipment (MicroMaxx, Sonosite, Bothell, WA) and analyzed by our research laboratory as previously described [17, 20].

Anonymized age-matched control and type 1 diabetic subjects' CMR data for a randomly selected pilot sub group (7 controls, 9 subjects with type 1 diabetes) were used to create subject-specific CFD models with fluid–structure interaction as described previously using SimVascular software package (https://simtk.org) and discretized using MeshSim (Simmetrix, Clifton Park, NY) [22]. Pulsatile flow waveforms from the measured ascending aortic CMR phase contrast data were applied as the inlet boundary condition for each CFD model using fully developed parabolic profiles [22]. To replicate the resistance to blood flow from vessels beyond CMR data, three-element Windkessel representations were imposed as outlet boundary conditions for each vascular branch using a coupled-multidomain method [42] as previously described [22]. This method provides an intuitive representation of the arterial tree beyond model outlets and can be described by three parameters with physiologic meaning: characteristic (i.e., regional) resistance (R_c), arterial capacitance (C), and distal resistance (R_d). Please see Table 1 for Windkessel parameters. The total arterial capacitance for each patient was determined from inflow (i.e., CMR phase contrast) and BP

measurements assuming a characteristic-to-total resistance ratio of 6 % [24]. The total arterial capacitance was then distributed among outlets according to their blood flow distributions [37] as measured by CMR phase contrast data of each aortic branch. Once the capacitance terms for each branch were assigned, the terminal resistance for each branch was calculated from mean BP (via DASH 3000) and flow (via CMR phase contrast) and distributed between the characteristic and distal resistance parameters by adjusting Rc:terminal resistance ratios (6–10 %) to replicate measured BP using the pulse pressure method [36]. This approach results in flow distributions and BP values within 5 % of the measured values.

Coupled blood flow and vessel wall dynamics were solved using a coupled-momentum method [7] formulation and parameters discussed in detail elsewhere [22]. Briefly, CFD models were initially pre-stressed by loading the vessel wall with the diastolic pressure, assuming that the geometry given by the collective SSFP images approximates a diastolic (i.e., reference) configuration. Literature

Table 1 Range of Windkessel and arterial parameters for the collection of CFD models in each group

	Control	T1DM
Young's modulus		
E (dyn/cm^2)	3.99E+06–3.57E+07	3.23E+06–1.17E+07
Innominate artery		
R_c (dynes/cm^5)	429–489	320–939
C (cm^5/dyn)	1.22E−04–1.42E−04	1.23E−04–3.99E−04
R_d (dynes/cm^5)	4,250–6,500	4,520–9,260
Left common carotid artery		
R_c (dynes/cm^5)	687–1,720	702–1,390
C (cm^5/dyn)	3.91E−05–1.15E−04	4.94E−05–1.52E−04
R_d (dynes/cm^5)	10,800–19,600	11,800–15,200
Left subclavian artery		
R_c (dynes/cm^5)	662–1,830	500–1,480
C (cm^5/dyn)	6.11E−05–1.26E−04	6.19E−05–1.62E−04
R_d (dynes/cm^5)	6,400–23,000	6,813–15,000
Descending aortic outlet		
R_c (dynes/cm^5)	99–231	101–232
C (cm^5/dyn)	2.67E−04–8.76E−04	2.84E−04–8.16E−04
R_d (dynes/cm^5)	894–4,580	1,530–4,710

E, Young's modulus; R_c, characteristic resistance; C, arterial capacitance; R_d, distal resistance

values for aortic thickness (0.15 cm), density (1.0 g/cm^3), and Poisson's ratio (0.5) were selected and Young's modulus, E, was adjusted iteratively until the ascending aortic (AAo) mean luminal displacement was within 5 % of the values from CMR phase contrast magnitude measurements. Please see Table 1 for the range of E used. This approach was previously found to provide reasonable wall displacement in simulations when compared to spatially equivalent locations from CMR phase contrast [22].

Time-dependent CFD simulations with fluid–structure interaction were performed using an in-house stabilized finite element method with an embedded commercial linear solver LESLIB (Altair Engineering, Troy, MI) to solve the conservation of mass (continuity), balance of fluid momentum (Navier–Stokes), and vessel wall elastodynamics equations [7]. Meshes contained >3 million tetrahedral elements and localized refinement was performed using an adaptive technique to deposit more elements in regions prone to flow disruption [28, 34], which has been previously described in detail elsewhere [21]. Simulations were run for 4–6 cardiac cycles until the flow rate and pressure fields yielded periodic solutions. For comparison with distensibility calculations, mean TAWSS and oscillatory shear index (OSI) values were then calculated within circumferential bands, where the thickness of the phase contrast imaging slice intersected the AAo and descending (DAo$_T$) aorta [22, 25]. TAWSS and OSI values were also extracted longitudinally along the inner and outer curvatures of the thoracic aorta, as well as along its anatomic right and left sides [23]. The location of the left subclavian artery (LSCA) was taken as the zero point for quantification, with all other aortic locations noted relative to this; aortic regions distal to the LSCA were given positive location designation and locations proximal (i.e., closer to the aortic valve) received a negative designation in terms of location [23].

Statistical Analyses

Medians and ranges are given for continuous demographic variables. Scatter plots and Pearson's correlation coefficients were used for the analyses of correlation between two measurements. A Mann–Whitney test was used to compare the controls and subjects with type 1 diabetes.

We did not adjust for multiple testing since the power of the study is low and adjustment would increase considerably an already high chance of a type II error.

Results

Twenty-eight subjects (age 15.7 years (11.6–18.4), 20 with type 1 diabetes age 15.8 years (11.6–18.4), and 8 controls

Table 2 Demographics

	Type 1 diabetic subjects ($n = 20$)[a]	Control subjects ($n = 8$)[a]
Age (years)	15.8 (11.6–18.4)	15.4 (10.3–18.2)
Gender	10 male (50 %)	5 male (62.5 %)
Age at diabetes diagnosis (years)	6.3 (1.1–11.1)	Not applicable
Diabetes duration (years)	9.4 (2.2–13. 5)	Not applicable
Body mass index (kg/m^2)	21.1 (14.0–34.0)	22.4 (17.3–34.3)
Body surface area (m^2)	1.72 (1.14–2.10)	1.74 (1.24–2.26)
Right arm systolic BP (mmHg)	114 (103–139)	118 (101–127)
Right arm diastolic BP (mmHg)	68 (59–77)	68 (56–78)
Heart rate (beats/min)	49 (37–58)	51 (39–74)

[a] Data displayed as median and ranges; no significant differences seen ($p > 0.05$)

(age 15.4 years (10.3–18.2)) were recruited from the Children's Hospital of Wisconsin. Subjects were of similar age, gender, and body habitus with no significant difference in resting BP (Table 2). Similarly, there were no differences in heart rate, cardiac output, or cardiac index between groups. Control subjects underwent clinical CMR scanning for the following indications: pectus excavatum (1 patient), to rule out arrhythmogenic right ventricular dysplasia (ARVD) (3 patients, with study negative for ARVD in all 3), very small ventricular septal defect (1 patient), repaired tetralogy of Fallot (1 patient), repaired pulmonary stenosis (1 patient), and anomalous origin of the right coronary artery from the left sinus of Valsalva (1 patient). Subjects with type 1 diabetes had disease for 9.4 (2.2–13.5) years, and all were taking insulin at time of recruitment. Two patients with diabetes were using levothyroxine and none were on lipid lowering medication at recruitment. Control subjects were not receiving chronic medications. Significant differences were seen between the controls and diabetic subjects for glucose, HgbA1c, and triglyceride level, but not for other venous blood values (Table 3).

Brachial artery reactivity data showed a significant difference for FMD% between control and diabetic subjects ($p = 0.036$) (Table 3). There was also a significant difference between control and diabetic subjects' ascending aortic distensibility ($p = 0.006$), but not distensibility in other regions of the aorta. FMD% positively correlated with age at diabetes diagnosis ($r = 0.468$, $p = 0.038$) and HgbA1c ($r = 0.472$, $p = 0.036$), and negatively with years post diagnosis ($r = -0.547$, $p = 0.013$). Brachial artery reactivity testing (FMD) did not correlate significantly with aortic distensibility or the TAWSS and OSI results for this

Table 3 Traditional Venous blood coronary artery disease risk factors and brachial artery measures of vascular health

	Type 1 diabetic subjects ($n = 20$)[a]	Control subjects ($n = 8$)[a]	p*
Total cholesterol (mg/dL)	162 (125–348)	158 (140–263)	NS
LDL (mg/dL)	88 (58–240)	90 (67–203)	NS
HDL (mg/dL)	56 (41–74)	58 (44–68)	NS
Triglycerides (mg/dL)	87 (45–298)	48 (34–118)	0.003
Glucose (mg/dL)	140 (76–366)	84 (80–98)	0.001
Insulin level (μU/mL)	4.0 (1–24)	3 (1–15)	NS
HgbA1c (mmol/mol)	62 (44–119)	33 (31–40), $n = 7$	< 0.001
Fibrinogen (mg/dL)	296 (216–464)	239 (203–365)	NS
hs-CRP (mg/L)	0.5 (0.1–22.4)	0.3 (0.1–2.4)	NS
Homocysteine (μmol/L)	4.9 (3.4–9.1), $n = 19$	6.0 (4.5–7.1), $n = 7$	NS
FMD % (EKG)	6.5 (1.9–13.6)	7.8 (6.6–9.7), $n = 7$	0.036
Distensibility[b] AAo	9.3 (4.3–17.2) $n = 19$	5.8 (3.1–9.5)	0.006
Distensibility[b] DAo$_T$	10.5 (4.0–20.0)	7.9 (4.6–17.5)	NS
Distensibility[b] DAo$_D$	12.6 (7.4–22.9), $n = 19$	9.5 (5.1–15.6), $n = 6$	NS

AAo ascending aorta, *DAo$_T$* descending mid thoracic aorta, *DAo$_D$* descending aorta at diaphragm, *NS* not significant

* $p > 0.05$

[a] Data displayed as median and ranges

[b] Distensibility was expressed as 10^{-3} mmHg^{-1}

pilot study, though interesting qualitative differences in TAWSS and OSI are apparent throughout the thoracic aorta (color images, Figs. 1, 2). Although no significant differences in global TAWSS or OSI were viewed for selected AAo or DAo$_T$ imaging planes, a trend toward significance existed for DAo$_T$ TAWSS, with diabetic patients having higher TAWSS than controls ($p = 0.072$) (Table 4). OSI distributions appeared similar between groups at this stage. Looking at a more granular level, for control subjects, the aorta had more local regions with low TAWSS (blue on color images), when compared to type 1 diabetic patients. Specifically, along right, left, outer and, to a lesser degree, the inner curvatures of the aorta, median TAWSS at each location for diabetics (denoted by the red line on the graphs) tended to be higher than median TAWSS for the controls (black line). These differences reached significance at two locations, one along the outer curvature (location 1.25) and another along the anatomic right side (location 1.5) of the aorta (Fig. 1). For OSI, significant differences are also seen in the area distal to the take-off of the LSCA (Fig. 2) at locations 1.5 and 2.0 along the outer curvature, and locations near 0.5 along the anatomic left side of the aorta. For this small sub group with CFD modeling, though, neither global nor regional aortic TAWSS correlated with any clinical or laboratory value for either the control or diabetic subjects. There was a significant correlation between control subjects' total cholesterol and global DAo$_T$ OSI ($r = 0.767$, $p = 0.044$). After excluding one diabetic outlier (where hs-CRP = 22), there was a trend toward a negative correlation between hs-CRP and AAo distensibility ($r = -0.459$, $p = 0.064$), but not distensibility in other areas, suggesting regional differences in aortic wall properties.

Discussion

Endothelial dysfunction is considered a key event in the development of atherosclerosis. Measures of endothelial dysfunction have included brachial artery reactivity testing, pulse wave velocity assessment by radial artery tonometry, and intimal-medial thickening assessment by ultrasound [14]. Impaired FMD response, by brachial artery reactivity testing, has been shown to detect endothelial dysfunction in subjects with hyperlipidemia (being especially affected by elevated total cholesterol), hypertension, and/or diabetes—traditional cardiovascular risk factors for CAD [5, 10, 18]. The impaired brachial artery reactivity seen in our cohort is similar to what has been seen by others. Babar et al. showed that pre-adolescent children with type 1 diabetes, and mean diabetes duration of 4 years, displayed evidence of low-intensity vascular inflammation and attenuated FMD measurements [3]. The positive correlations seen in the present research between FMD and subject age at diabetes diagnosis, years with diabetes, and HgbA1c, are congruent with the literature [13]; vascular health worsens with duration of poor glucose control. Furthermore, early autonomic derangements have been observed in patients with type 1 diabetes and are believed to be functional and irreversible [33]. Although we did not assess the role of sympathetic nervous system (SNS) activity on FMD, increased SNS activity has not been shown to blunt FMD response [6].

The novelty of our pilot research is in the application of CMR to this young cohort of patients with type 1 diabetes to look at early vascular changes. No literature exists for the study of CMR CFD modeling with fluid–structure interaction for young diabetic patients. Functional
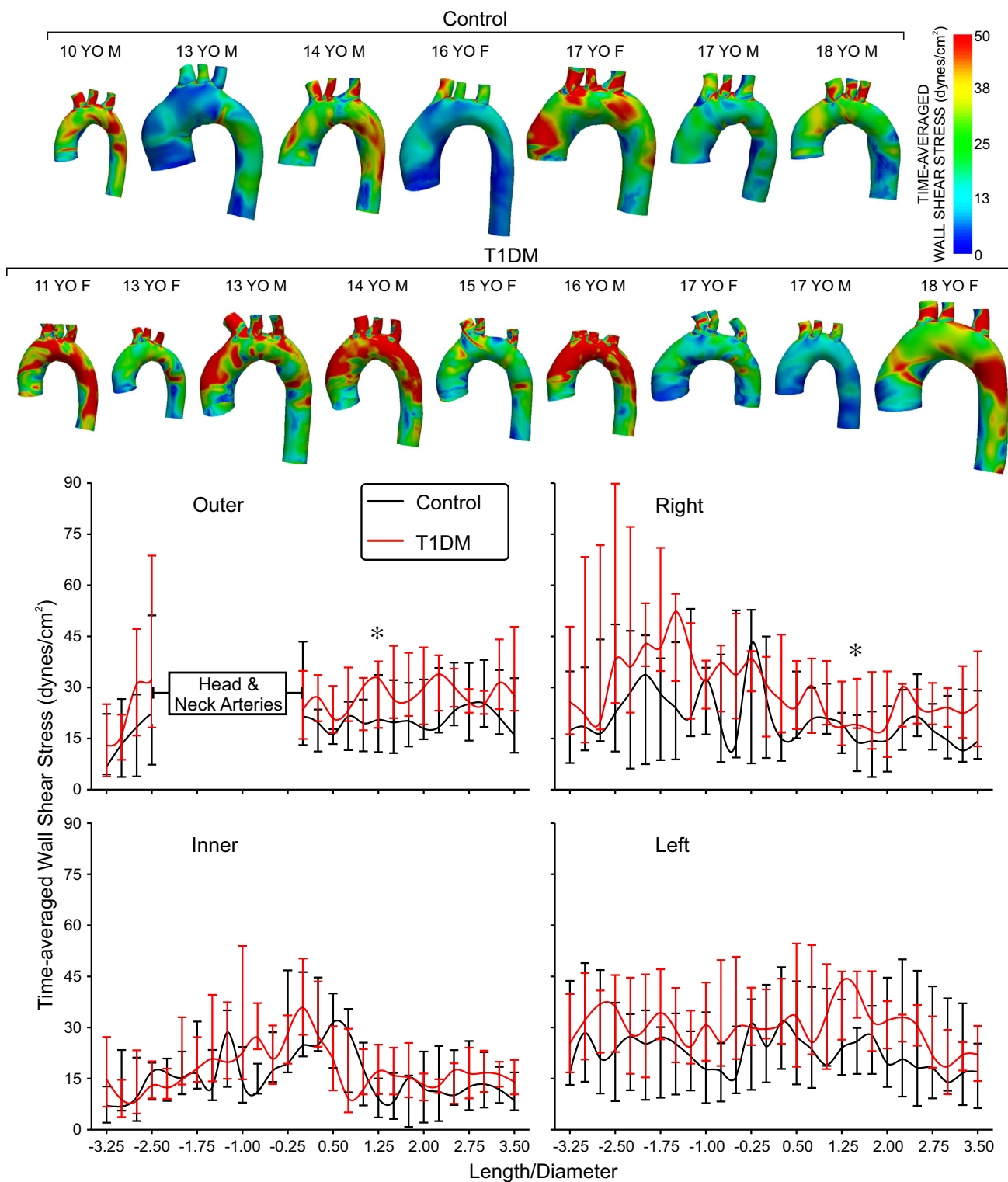
assessment of thoracic aortic properties such as aortic stiffness by CMR has been validated [27, 32]. Aquaro et al. [2], studying 85 healthy subjects (ages 15 to greater than 60 years) by CMR, showed that there is progressive impairment of the elastic properties of the aortic wall with aging (i.e., maximum rate of systolic distension and distensibility decrease progressively through with age ($p < 0.001$) and pulse wave velocity increased). Others have applied this technique to the study of patients with chronic renal disease, where increased arterial stiffness has

◄**Fig. 1** Collective time-averaged wall shear stress (TAWSS) distributions from CFD (*top*) and ensemble-averaged, longitudinal TAWSS distributions comparing CFD models for seven control subjects (*black*) and nine age- and gender-matched type 1 diabetic subjects (*red*) along the outer, anatomic right, anatomic left, and inner curvatures of the aorta (*bottom*). The x-axis denotes location along the arch divided by the diameter at the outlet of each patient's model. This approach accounts for differences in aortic dimensions resulting from differences in size between patients and was used to normalize the longitudinal locations among all patients. The left subclavian artery (LSCA) was then taken as the zero point for quantification, with all other aortic locations noted relative to this. Hence, aortic regions distal to the LSCA have a positive location designation and locations proximal (i.e., closer to the aortic valve) have a negative designation in terms of their location. Statistically different values exist when compared to control subjects (*$p < 0.05$). Data are expressed as medians with *bars* representing lower and upper quartiles

been associated with mortality in patients with chronic kidney disease. Aortic distensibility, measured by CMR using the methods employed here, was an independent predictor of combined vascular events and mortality in this study of chronic renal patients. Furthermore, AD predicted all cause mortality [26].

Our pilot study is unique in its use of CMR to study the central vasculature in a young diabetic population at risk for premature atherosclerosis, showing that it is feasible to characterize differences in their central vasculature when compared with controls. Regional TAWSS derived from patient-specific CFD modeling appeared qualitatively different for type 1 diabetic subjects when compared with controls (Fig. 1). Vascular changes appear heterogeneous in the youthful cohorts studied here; in this early phase, the impact of regional TAWSS may not be detected by the more global measure of CMR aortic distensibility measured at one or two aortic locations (AAo and DAo_T). This altered vascular TAWSS may become more widespread throughout the aorta with patient aging, the subject of future, powered, longitudinal study.

Low TAWSS is thought, from studies of adult subjects, to promote atherogenesis, as is elevated OSI, an index of directional changes in wall shear stress. The importance of these parameters and their serial change with aging, though, is not known. In our study of young type 1 diabetic patients, it appears that regional differences in TAWSS exist when compared with controls and that higher TAWSS is seen in the ascending aorta, reaching significance for several locations the transverse arch. In theory this could be explained by differences in CFD simulation boundary conditions, but cardiac output, cardiac index, flow distributions to aortic branches, heart rate and the portion of the period spent in systole did not differ between groups. Many cardiovascular risk factors, including type 1 diabetes, induce physiological outward arterial remodeling (dilation) that begins in response to overall higher initial laminar

shear stress (Glagov phenomenon). As the vessels become inflamed, remodeling becomes excessive, and the result is adverse shear stress in larger arteries [30]. In our study of young patients, it is possible we are seeing this early remodeling, where wall shear stress is still high and the aorta, which has begun to stiffen, has yet to dilate. Moreover, extension of the endothelial dysfunction observed in this pilot study could prevent myogenic dilation in response to elevated TAWSS. Chronic and sustained increased TAWSS may further contribute to endothelial dysfunction, which also progresses with age. Serial data, while not part of the current study, may show that TAWSS changes with age, such that at the point of adulthood, when plaque is apparent, TAWSS levels have transitioned and are low.

Mean ascending aortic distensibility for our type 1 diabetic cohort ($9.8 \pm 2.7 \times 10^{-3}$ mmHg^{-1}) differed from controls ($6.2 \pm 2.4 \times 10^{-3}$ mmHg^{-1}, $p = 0.006$). At first glance, this implies a paradoxically more compliant aorta for the diabetic cohort; yet upon further review, all values for diabetic subjects fall well within published normal range, where for ages 15–20 years, females have aortic distensibility $13.2 \pm 3.4 \times 10^{-3}$ mmHg^{-1} (range 8.3–16.3) and males $8.1 \pm 2.9 \times 10^{-3}$ mmHg^{-1} (range 6.5–12.7) [2, 43]. Published variability in this measure shows a mean difference (±standard error, SE) of 3 % (±7 %) with 95 % confidence interval (CI) for limits of agreement of ±69 % [8]. Thus, the differences in AAo distensibility seen here are not clinically meaningful. The diabetic cohort's CFD modeling, though, shows that there already appear to be regional differences in TAWSS, supporting the notion that CFD modeling may be a more sophisticated method to assess regional vascular changes than is distensibility.

When compared with aortic distensibility in adult diabetic patients (ages 48–64 years), where distensibility of the aorta was lowest (~ 3.8–4×10^{-3} mmHg^{-1}) versus adult controls without disease ($\sim 5 \times 10^{-3}$ mmHg^{-1}), $p = 0.011$, our diabetic subjects' aortic distensibility, though, appears better—as would be expected for this younger group [35]. Arterial distensibility decreases with age, with increased wall stiffness of the proximal aorta seen with increased age [1]. The decreasing aortic elasticity, observed with aging, has been related to normal structural wall changes during aging, including increased intimal-medial thickness beginning after birth and to the cycles of contraction and expansion of the vasculature in response to cardiac systole which fragments elastic fibers in the wall, transferring of stress stiff collagen fibers [43].

Correlations seen here between reduced aortic distensibility and elevated venous biomarkers (elevated homocysteine, HgbA1c, and hs-CRP) speak to the biochemical milieu which invokes inflammatory mechanisms involved
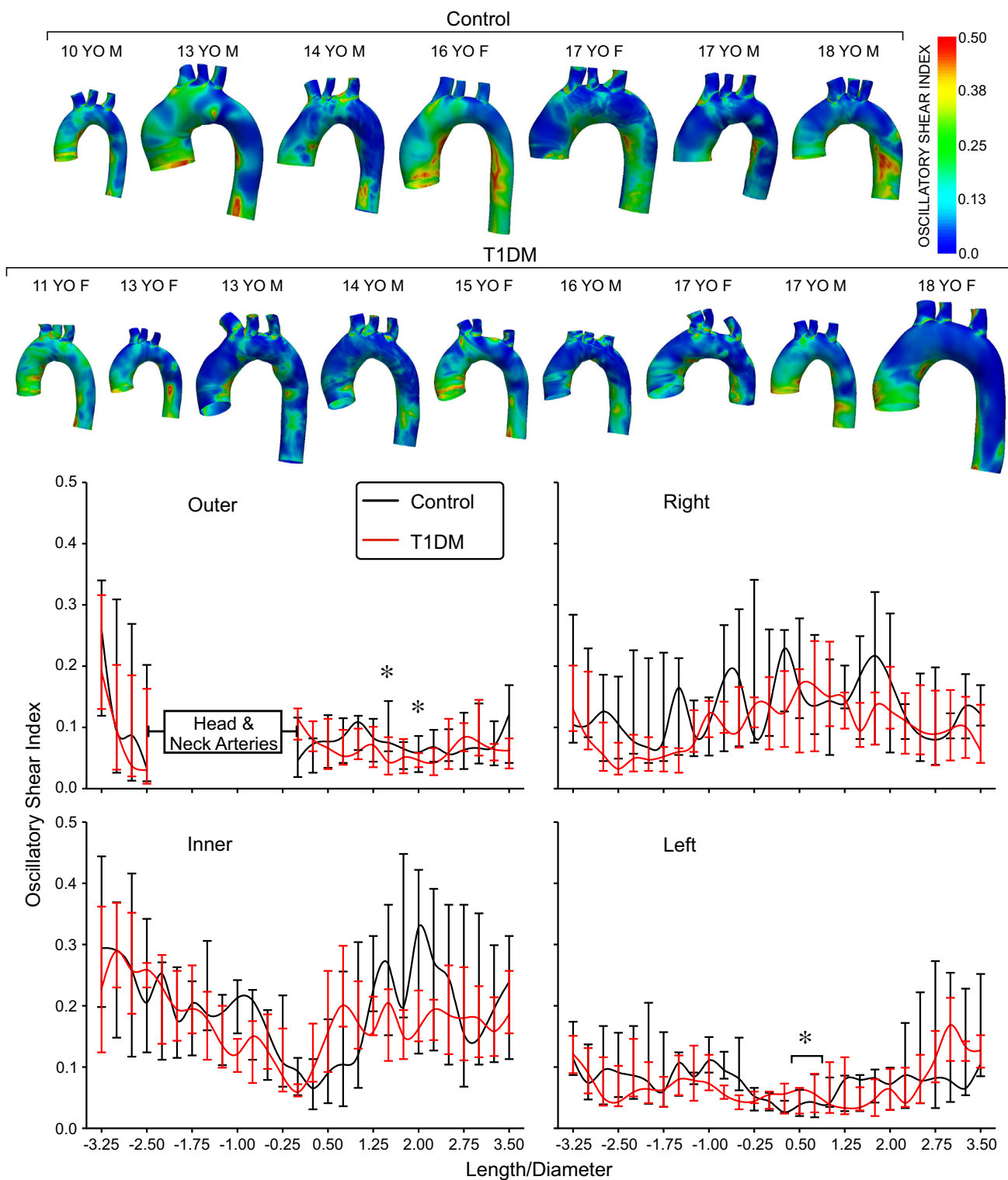
Fig. 2 Collective oscillatory shear index (OSI) distributions from CFD (*top*) and ensemble-averaged, longitudinal aortic OSI distributions comparing CFD models for seven control subjects (*black*) and nine age- and gender-matched type 1 diabetic subjects (*red*) along the outer, anatomic right, anatomic left, and inner curvatures of the aorta (*bottom*). The *x*-axis denotes location along the arch divided by the diameter at the outlet of each patient's model. This approach accounts for differences in aortic dimensions resulting from differences in size between patients and was used to normalize the longitudinal locations among all patients. The LSCA was then taken as the zero point for quantification, with all other aortic locations noted relative to this. Hence, aortic regions distal to the LSCA have a positive location designation and locations proximal (i.e., closer to the aortic valve) have a negative designation in terms of their location. Statistically different values exist when compared to control subjects (*$p < 0.05$). Data are expressed as medians with bars representing lower and upper quartiles

Table 4 Novel measures of vascular health from CFD modeling

	Type 1 diabetes subjects ($n = 9$)[a]	Control subjects ($n = 7$)[a]	$p*$
TAWSS AAo (dynes/cm^2)	20.4 (6.1–38.8)	16.8 (7.5–35.4)	0.832
TAWSS DAo$_T$ (dynes/cm^2)	28.6 (8.6–39.0)	17.9 (10.2–28.4)	0.072
OSI AAo	0.16 (0.13–0.28)	0.18 (0.10–0.23)	0.916
OSI DAo$_T$	0.12 (0.06–0.16)	0.15 (0.10–0.19)	0.244

A Ao ascending aorta, *DAo$_T$* descending mid thoracic aorta

* No significant differences seen ($p > 0.05$)

[a] Data displayed as median and ranges

in the development of endothelial dysfunction. The regional nature of these correlations between aortic distensibility and venous biomarkers is not unexpected, given the heterogeneous vascular changes seen on CFD modeling. From a basic science perspective, hyperhomocysteinemia has been shown to induce smooth muscle cell proliferation, endothelial dysfunction, collagen synthesis, and deterioration of elastic material of the arterial wall [39]. Elevated plasma homocysteine has been shown to increase the risk of atherothrombosis, especially in individuals with impaired glucose tolerance [16] and pediatric type 1 diabetic populations with micro albuminuria [47]. The role of elevated hs-CRP in all stages of atherogenesis, including endothelial dysfunction, atherosclerotic plaque formation, plaque maturation, plaque destabilization, and eventual rupture, is well known [48]. Subjects with type 1 diabetes and control subjects had similar homocysteine and hs-CRP in our pediatric pilot study suggesting early disease (or perhaps reflecting small sample size).

Limitations

This was a prospective, pilot study funded by an investigational grant; thus, subject enrollment was limited by available funding. Control subjects were chosen from those with clinically indicated CMR scans, rather than imaging "healthy children." Careful attention was paid, though, to avoid those with congenital heart disease affecting the aorta; in fact, in four controls, no cardiac disease existed at all, as ARVD was not found (3) and pectus chest wall deformity did not affect the heart (1). One patient with repaired tetralogy of Fallot (a 13-year-old male) served as a control subject early in the course of this study. His left ventricular outflow tract was normal and he had only trace aortic regurgitation with aortic dimensions just slightly above the normal range [19]. The authors subsequently

recognized that subsequent such subjects should not be permitted as controls. Furthermore, the cross-sectional nature of the study allows characterization of the population, but limits comment on the longitudinal significance of aortic distensibility and regional TAWSS and OSI.

CMR images for selected three-dimensional SSFP whole heart acquisitions were performed with the patient breathing comfortably and with acquisition navigated off the position of the diaphragm; as such, these were time-consuming (10–15 min acquisition time) acquisitions, leading to slight degradation in image quality for the descending aorta near the diaphragm, truncating some CFD models (Figs. 1, 2). Three-dimensional data acquired with gadolinium (Gd) dye (used for clinically indicated scans in controls) preserved image quality. As Gd does not have Food and Drug Administration approval for cardiac imaging, it was not used for diabetic subjects, but only for cases where its use was clinically indicated (controls). While this difference in technique for acquisition of the 3D aortic data set is a study limitation, others have shown that there is no significant difference in the orthogonal measurements of the aortic diameter between those made on images from the 3D SSFP and those made from the contrast enhanced MRA sequences [9].

Assumptions exist with CFD modeling which relies on definition of inlet and outlet boundary conditions, as discussed in detail elsewhere (17). CFD results were considered mesh independent when TAWSS at several regions in the aorta changed <1 % between successive simulations. Thus, while it is possible that the results presented may differ for much larger meshes, it is unlikely that the key observations would be altered. Inclusion of the AoV with CFD simulations has been shown to impact hemodynamics, but was not employed [45], because valvular imaging was not conducted when the imaging data was collected.

In conclusion, while global measures of aortic distensibility obtained by CMR show no clinically meaningful differences when young diabetic patients are compared with controls (with both having aortic distensibility within the normal range), CFD determined regional TAWSS and OSI data appear qualitatively different. For outer and right curvatures of the transverse aorta (just proximal to the origin of the LSCA), TAWSS and OSI were significantly different for diabetics versus controls. CFD modeling, thus, shows promise as a method of elucidating the early regional vascular changes in the aortic wall, when exposed to biochemical stresses of type 1 diabetes. Longitudinal CMR studies of children and young adults are warranted to better understand these vascular changes and the cardiac burden imposed by type 1 diabetes.

References

1. Aggoun Y, Szezepanski I, Bonnet D (2005) Noninvasive assessment of arterial stiffness and risk of atherosclerotic events in children. Pediatr Res 58:173–178. doi:10.1203/01.PDR.0000170900.35571.CB

2. Aquaro GD, Cagnolo A, Tiwari KK, Todiere G, Bevilacqua S, Di Bella G, Ait-Ali L, Festa P, Glauber M, Lombardi M (2013) Age-dependent changes in elastic properties of thoracic aorta evaluated by magnetic resonance in normal subjects. Interact Cardio-Vasc Thorac Surg 17:674–679. doi:10.1093/icvts/ivt261

3. Babar GS, Zidan H, Widlansky ME, Das E, Hoffmann RG, Daoud M, Alemzadeh R (2011) Impaired endothelial function in preadolescent children with type 1 diabetes. Diabetes Care 34:681–685. doi:10.2337/dc10-2134

4. Celermajer DS, Sorensen KE, Gooch VM, Spiegelhalter DJ, Miller OI, Sullivan ID, Lloyd JK, Deanfield JE (1992) Noninvasive detection of endothelial dysfunction in children and adults at risk of atherosclerosis. Lancet 340:1111–1115

5. De Michele M, Iannuzzi A, Salvato A, Pauciullo P, Gentile M, Iannuzzo G, Panico S, Pujia A, Bond GM, Rubba P (2007) Impaired endothelium-dependent vascular reactivity in patients with familial combined hyperlipidaemia. Heart 93(1):78–81. doi:10.1136/hrt.2006.093278

6. Dyson KS, Shoemaker JK, Hughson RL (2006) Effect of acute sympathetic nervous system activation on flow-mediated dilation of brachial artery. Am J Physiol Heart Circ Physiol 290:H1446–H1453

7. Figueroa CA, Vignon-Clementel IE, Jansen KE, Hughes TJR, Taylor CA (2006) A coupled momentum method for modeling blood flow in three-dimensional deformable arteries. Comput Methods Appl Mech Eng 195:5685–5706. doi:10.1016/j.cma.2005.11.011

8. Forbat SM, Mohiaddin RH, Yang GZ, Firmin DN, Underwood SR (1995) Measurement of regional aortic compliance by MR imaging: a study of reproducibility. J Magn Reson Imaging 5:635–639. doi:10.1002/jmri.1880050604

9. Francois CJ, Tuite D, Deshpande V, Jerecic R, Weale P, Carr J (2008) Unenhanced MR angiography of the thoracic aorta: initial clinical evaluation. Am J Roentgenol 190(4):902–906. doi:10.2214/AJR.07.2997

10. Ghiadoni L, Huang Y, Magagna A, Buralli S, Taddei S, Salvetti A (2001) Effect of acute blood pressure reduction on endothelial function in the brachial artery of patients with essential hypertension. J Hypertens 19(3 Pt 2):547–551

11. Go AS, Mozaffarian D, Roger VL, Benjamin EJ, Berry JD, Blaha MJ, Dai S, Ford ES, Fox CS, Franco S, Fullerton HJ, Gillespie C, Hailpern SM, Heit JA, Howard VJ, Huffman MD, Judd SE, Kissela BM, Kittner SJ, Lackland DT, Lichtman JH, Lisabeth LD, Mackey RH, Magid DJ, Marcus GM, Marelli A, Matchar DB, McGuire DK, Mohler ER, Moy CS, Mussolino ME, Neumar RW, Nichol G, Pandey DK, Paynter NP, Reeves MJ, Sorlie PD, Stein J, Towfighi A, Turan TN, Virani SS, Wong ND, Woo D, Turner MB (2014) Heart Disease and stroke statistics—2014 update: a report from the American Heart Association. Circulation 129:e28–e292. doi:10.1161/01.cir.0000441139.02102.80

12. Goldberg RB, Mellies MJ, Sacks FM, Moyé LA, Howard BV, Howard WJ, Davis BR, Cole TG, Pfeffer MA, Braunwald E, for the CARE Investigators (1998) Cardiovascular events and their reduction with pravastatin in diabetic and glucose-intolerant myocardial infarction survivors with average cholesterol levels: subgroup analyses in the cholesterol and recurrent events (CARE) trial. Circulation 98:2513–2519. doi:10.1161/01.CIR.98.23.2513

13. Grzelak P, Czupryniak L, Olszycki M, Majos A, Stefańczyk L (2011) Age effect on vascular reactivity in type 1 diabetes. Diabet Med 28(7):833–837. doi:10.1111/j.1464-5491.2011.03277.x

14. Haller MJ, Samyn M, Nichols WW, Brusko T, Wasserfall C, Schwartz RF, Atkinson M, Shuster JJ, Pierce GL, Silverstein JH (2004) Radial artery tonometry demonstrates arterial stiffness in children with type 1 diabetes. Diabetes Care 27:2911–2917. doi:10.2337/diacare.27.12.2911

15. Herman WH, Alexander CM, Cook JR, Boccuzzi SJ, Musliner TA, Pedersen TR, Kjekshus J, Pyörälä K (1999) Effect of simvastatin treatment on cardiovascular resource utilization in impaired fasting glucose and diabetes. Findings from the Scandinavian Simvastatin Survival Study. Diabetes Care 22:1771–1778. doi:10.2337/diacare.22.11.1771

16. Hoogeveen EK, Kostense PJ, Beks PJ, Mackaay AJC, Jakobs C, Bouter LM, Heine RJ, Stehouwer CDA (1998) Hyperhomocysteinemia is associated with an increased risk of cardiovascular disease, especially in non-insulin-dependent diabetes mellitus: a population-based study. Arterioscler Thromb Vasc Biol 18:133–138. doi:10.1161/01.ATV.18.1.133

17. Järvisalo MJ, Rönnemaa T, Volanen I, Kaitosaari T, Kallio K, Hartiala JJ, Irjala K, Viikari JS, Simell O, Raitakari OT (2002) Brachial artery dilatation responses in healthy children and adolescents. Am J Physiol Heart Circ Physiol 282:H87–H92

18. Johnstone MT, Creager SJ, Scales KM, Cusco JA, Lee BK, Creager MA (1993) Impaired endothelium-dependent vasodilation in patients with insulin-dependent diabetes mellitus. Circulation 88(6):2510–2516. doi:10.1161/01.cir.88.6.2510

19. Kaiser T, Kellenberger CJ, Albisetti M, Bergstrasser E, Valsangiacomo Buechel ER (2008) Normal values for aortic diameters in children and adolescents-assessment in vivo by contrast enhanced CMR-angiography. J Cardiovas Magn Reson 10:56. doi:10.1186/1532-429X-10-56

20. Kizhakekuttu TJ, Gutterman DD, Phillips SA, Jurva JW, Arthur EI, Das E, Widlansky ME (2010) Measuring FMD in the brachial artery: how important is QRS gating? J Appl Physiol 109:959–965. doi:10.1152/japplphysiol.00532.2010

21. Kwon S, Feinstein JA, Dholakia RJ, LaDisa JF Jr (2014) Quantification of local hemodynamic alterations cuased by virtual implantation of three commercially available stents for treatment of aortic coarctation. Pediatr Cardiol 35(4):732–740. doi:10.1007/s00246-013-0845-7

22. LaDisa JFJ, Figueroa CA, Vignon-Clementel I, Kim HJ, Xiao N, Ellwein LM, Chan FP, Feinstein JA, Taylor CA (2011) Computational simulations for aortic coarctation: representative results from a sampling of patients. J Biomech Eng 133:091008. doi:10.1115/1.4004996

23. LaDisa JFJ, Dholakia RJ, Figueroa CA, Vignon-Clementel IE, Chan FP, Samyn MM, Cava JR, Taylor CA, Feinstein JA (2011) Computational simulations demonstrate altered wall shear stress in aortic coarctation patients treated by resection with end-to-end

anastomosis. Congenit Heart Dis 6:432–443. doi:10.1111/j.1747-0803.2011.00553.x

24. Laskey WKP (1990) Estimation of total systemic arterial compliance in humans. J Appl Physiol 69:112–119

25. Les A, Shadden S, Figueroa CA, Park J, Tedesco M, Herfkens R, Dalman R, Taylor C (2010) Quantification of hemodynamics in abdominal aortic aneurysms during rest and exercise using magnetic resonance imaging and computational fluid dynamics. Ann Biomed Eng 38:1288–1313. doi:10.1007/s10439-010-9949-x

26. Mark P, Doyle A, Blyth K, Patel R, Weir R, Steedman T, Foster J, Dargie H, Jardine A (2008) Vascular function assessed with cardiovascular magnetic resonance predicts survival in patients with advanced chronic kidney disease. J Cardiovasc Magn Reson 10:39. doi:10.1186/1532-429X-10-39

27. Mohiaddin RHF (1993) Age-related changes of human aortic flow wave velocity measured noninvasively by magnetic resonance imaging. J Appl Physiol 74:492–497

28. Müller J, Sahni O, Li X, Jansen KE, Shephard MS, Taylor CA (2005) Anisotropic adaptive finite element method for modelling blood flow. Comput Methods Biomech Biomed Eng 8:295–305. doi:10.1080/10255840500264742

29. National Cholesterol Education Program (NCEP) (1992) Highlights of the report of the expert panel on blood cholesterol levels in children and adolescents. Pediatrics 89:495

30. Pasterkamp G, Galis ZS, de Kleijn DPV (2004) Expansive arterial remodeling: location, location, location. Arterioscler Thromb Vasc Biol 24:650–657. doi:10.1161/01.ATV.0000120376.09047.fe

31. Raitakari OT, Pitkänen O, Lehtimäki T, Lahdenperä S, Iida H, Ylä-Herttuala S, Luoma J, Mattila K, Nikkari T, Taskinen M, Viikari JSA, Knuuti J (1997) In vivo low density lipoprotein oxidation relates to coronary reactivity in young men. J Am Coll Cardiol 30:97–102. doi:10.1016/S0735-1097(97)00103-4

32. Redheuil A, Yu W, Wu CO, Mousseaux E, de Cesare A, Yan R, Kachenoura N, Bluemke D, Lima JAC (2010) Reduced ascending aortic strain and distensibility: earliest manifestations of vascular aging in humans. Hypertension 55:319–326. doi:10.1161/HYPERTENSIONAHA.109.141275

33. Rosengård-Bärlund M, Bernardi L, Fagerudd J, Mäntysaari M, Af-Björkesten CG, Lindholm H, Forsblom C, Wadé NJ, Groop P-H (2009) Early autonomic dysfunction in type 1 diabetes: a reversible disorder? Diabetologia 52:1164–1172. doi:10.1007/s00125-009-1340-9

34. Sahni O, Müller J, Jansen KE, Shephard MS, Taylor CA (2006) Efficient anisotropic adaptive discretization of the cardiovascular system. Comput Methods Appl Mech Eng 195:5634–5655. doi:10.1016/j.cma.2005.10.018

35. Soljanlahti S, Autti T, Hyttinen L, Vuorio AF, Keto P, Lauerma K (2008) Compliance of the aorta in two diseases affecting vascular elasticity, familial hypercholesterolemia and diabetes: a MRI study. Vasc Health Risk Manag 4:1103–1109. doi:10.2147/VHRM.S3198

36. Stergiopulos NS (1999) Use of pulse pressure method for estimating total arterial compliance in vivo. Am J Physiol Heart Circ Physiol 276:H424–H428

37. Stergiopulos N, Young DF, Rogge TR (1992) Computer simulation of arterial flow with applications to arterial and aortic stenoses. J Biomech 25:1477–1488. doi:10.1016/0021-9290(92)90060-E

38. Taniguchi H, Momiyama Y, Fayad ZA, Ohmori R, Ashida K, Kihara T, Hara A, Arakawa K, Kameyama A, Noya K, Nagata M, Nakamura H, Ohsuzu F (2004) In vivo magnetic resonance evaluation of associations between aortic atherosclerosis and both risk factors and coronary artery disease in patients referred for coronary angiography. Am Heart J 148:137–143. doi:10.1016/j.ahj.2004.03.008

39. Tawakol A, Omland T, Gerhard M, Wu JT, Creager MA (1997) Hyperhomocyst(e)inemia is associated with impaired endothelium-dependent vasodilation in humans. Circulation 95:1119–1121. doi:10.1161/01.CIR.95.5.1119

40. The Diabetes Atorvastatin Lipid Intervention (DALI) Study Group (2001) The effect of aggressive versus standard lipid lowering by atorvastatin on diabetic dyslipidemia: the DALI study: a double-blind, randomized, placebo-controlled trial in patients with type 2 diabetes and diabetic dyslipidemia. Diabetes Care 24:1335–1341. doi:10.2337/diacare.24.8.1335

41. Toikka JO, Niemi P, Ahotupa M, Niinikoski H, Viikari JSA, Rönnemaa T, Hartiala JJ, Raitakari OT (1999) Large-artery elastic properties in young men: relationships to serum lipoproteins and oxidized low-density lipoproteins. Arterioscler Thromb Vasc Biol 19:436–441. doi:10.1161/01.ATV.19.2.436

42. Vignon-Clementel IE, Figueroa CA, Jansen KE, Taylor CA (2006) Outflow boundary conditions for three-dimensional finite element modeling of blood flow and pressure in arteries. Comput Methods Appl Mech Eng 195:3776–3796. doi:10.1016/j.cma.2005.04.014

43. Voges I, Jerosch-Herold M, Hedderich J, Pardun E, Hart C, Gabbert D, Hansen J, Petko C, Kramer H, Rickers C (2012) Normal values of aortic dimensions, distensibility, and pulse wave velocity in children and young adults: a cross-sectional study. J Cardiovasc Magn Reson 14:77. doi:10.1186/1532-429X-14-77

44. Ward MR, Pasterkamp G, Yeung AC, Borst C (2000) Arterial remodeling: mechanisms and clinical implications. Circulation 102:1186–1191. doi:10.1161/01.CIR.102.10.1186

45. Wendell DC, Samyn MM, Cava JR, Ellwein LM, Krolikowski MM, Gandy KL, Pelech AN, Shadden SC, LaDisa JF Jr (2013) Including aortic valve morphology in computational fluid dynamics simulations: initial findings and application to aortic coarctation. Med Eng Phys 35:723–735. doi:10.1016/j.medengphy.2012.07.015

46. Wentzel JJ, Corti R, Fayad ZA, Wisdom P, Macaluso F, Winkelman MO, Fuster V, Badimon JJ (2005) Does shear stress modulate both plaque progression and regression in the thoracic aorta? Human study using serial magnetic resonance imaging. J Am Coll Cardiol 45:846–854. doi:10.1016/j.jacc.2004.12.026

47. Wotherspoon F, Laight DW, Browne DL, Turner C, Meeking DR, Allard SE, Munday LJ, Shaw KM, Cummings MH (2006) Plasma homocysteine, oxidative stress and endothelial function in patients with type 1 diabetes mellitus and microalbuminuria. Diabet Med 23:1350–1356. doi:10.1111/j.1464-5491.2006.01980.x

48. Yasmin CMM, Wallace S, Mackenzie IS, Cockcroft JR, Wilkinson IB (2004) C-reactive protein is associated with arterial stiffness in apparently healthy individuals. Arterioscler Thromb Vasc Biol 24:969–974. doi:10.1161/01.ATV.zhq0504.0173